

Original Research

Construction and Validation of a Prognostic Model of Metabolism-Related Genes Driven by Somatic Mutation in Bladder Cancer

Liang Wei¹, Lina Ji^{2,3}, Shuaihong Han¹, Mingquan Xu¹, Xiaofeng Yang^{1,*}¹Department of Urology, First Hospital of Shanxi Medical University, 030001 Taiyuan, Shanxi, China²Cancer Center, Shanxi Bethune Hospital, Shanxi Academy of Medical Sciences, Tongji Shanxi Hospital, Third Hospital of Shanxi Medical University, 030032 Taiyuan, Shanxi, China³Cancer Center, Tongji Hospital, Tongji Medical College, Huazhong University of Science and Technology, 430030 Wuhan, Hubei, China*Correspondence: tgbz116@126.com (Xiaofeng Yang)

Academic Editor: Fu Wang

Submitted: 30 January 2023 Revised: 8 May 2023 Accepted: 18 May 2023 Published: 19 October 2023

Abstract

Background: Metabolic reprogramming is an important player in the prognosis of cancer patients. However, metabolism-related genes (MRGs) that are essential to the prognosis of bladder cancer (BLCA) are not yet fully understood. The purpose of this study is to use bioinformatics methods to establish prognostic models based on MRGs in BLCA to screen potential biomarkers. **Methods:** Based on the transcriptomic data from BLCA patients in The Cancer Genome Atlas Program (TCGA) and Gene Expression Omnibus (GEO) databases, we identified the differentially expressed genes related to metabolism and analyzed the functional enrichment by edgeR package. A prognostic model was generated using univariate Cox regression analysis and validated using GEO dataset. The prognostic risk model was analyzed by the Kaplan-Meier curve. The single cell RNA sequencing (scRNA-seq) revealed the gene interaction networks and traced the development trajectories of distinct cell lineages. The levels of key metabolism-related biomarkers *in vitro* were verified by quantitative real-time polymerase chain reaction (qRT-PCR). **Results:** We screened 201 differentially expressed metabolism-related genes (DEMGRs), which were significantly enriched in oxidative phosphorylation. The risk model was constructed by 5 biomarkers. qRT-PCR analysis verified that there is a significant higher expression of *FASN* and *MTHFD1L* in carcinoma tissue. **Conclusions:** This study constructed a novel prognostic model based on a combination of clinical and molecular factors that related to metabolic reprogramming, which has the potential to improve the prediction of independent prognosis indicators and management of BLCA patients, leading to better treatment outcomes and survival rates.

Keywords: bladder cancer; metabolism-related genes; somatic mutations; prognostic model; biomarkers; single-cell analysis

1. Introduction

Bladder cancer (BLCA) is one of the most invasive malignant tumors in the urinary system, and it is associated with a high recurrence rate and high mortality rate [1]. In 2020, there were 573,000 new cases and 213,000 deaths worldwide [2]. Urothelial cancer, is the most common type of BLCA, accounting for 95% of cases. It is typically classified into two main subtypes based on the depth of invasion into the bladder wall: non-muscular invasive bladder cancer (NMIBC) and muscular invasive bladder cancer (MIBC). The treatment for BLCA depends on the stage and grade of the tumor, and the main treatment options include transurethral resection of bladder tumor, intravesical instillation, radical cystectomy, chemotherapy, radiotherapy, immunotherapy, and targeted therapy [3,4]. Although there are various therapy methods that have made great progress, more than half of the patients may still relapse or progress after treatment, and the cystectomy rate and cancer-specific mortality rate of these patients are significantly higher. It is a serious threat to the quality of life and even the lives of patients with BLCA [5,6]. One of

the reasons may be the lack of reliable biomarkers to accurately predict the prognosis and the inability to stratify the risk in advance, which makes it impossible for us to adjust the treatment plan accordingly [7].

Studies have indicated that all kinds of cancer cells undergo great metabolic changes in order to maintain their proliferation and evolution under adverse environment, mainly as follows: glucose metabolism dominated by aerobic glycolysis, oxidative phosphorylation weakened, pentose phosphate metabolic pathway enhanced, glutamine catabolism active, fatty acid ab initio synthesis and β -oxidation active [8,9]. These metabolic changes are called metabolic reprogramming, which is one of the markers of cancer cells [10] and a critical factor in regulating the formation and progression of cancer [11]. At the same time, the accumulation of somatic gene mutations results in the occurrence and development of cancer, and some of these gene mutations will induce metabolic reprogramming of newborn tumor cells to obtain these metabolic characteristics that support their survival, evade immune surveillance and proliferative growth, and constantly adapt to the dy-



dynamic tumor microenvironment [12]. Therefore, it is great significance to in-depth study of these somatic mutation-driven cancer metabolism-related genes (MRGs), which would lead to the development of potential biomarkers for early diagnosis and prognosis, as well as new therapeutic targets and approaches.

Previous studies have confirmed that some MRGs are closely associated with the occurrence and progression of BLCA. Fructose-1 receptor 6-diphosphatase 1 (FBP1), as a potential biomarker of BLCA molecular subtypes, is involved in glycolysis flow and gluconeogenesis [13]. Fork frame transcription factor J1 (FOXJ1) also plays a role in glycolysis phenotype of BLCA [14]. Furthermore, fatty acid desaturase 1 (FADS1), which is a member of the fatty acid desaturase gene family, has been shown that its over-expression is positively correlated with BLCA tumor grade [15]. The epigenetic crosstalk of *SAT1* and *ASS1* genes might play a role in chemotherapy and personalized treatment of BLCA by regulating the amino acid metabolism of BLCA [16]. While certain MRGs have been shown to be associated with BLCA, the potential value of these genes in predicting the prognosis of BLCA independently is limited. Furthermore, the important role of somatic mutation is not included in the research system, which requires us to further develop and explore.

The development of single cell sequencing (scRNA-seq) technology has given us a new and profound understanding of cancer evolution, tumor microenvironment (TME) and tumor heterogeneity. This has led to new insights into the mechanisms of tumorigenesis, tumor metastasis, and therapeutic resistance, and has helped identify novel drug targets and treatment strategies [17]. For example, the application of scRNA-seq in the field of BLCA has enhanced our understanding of the origin and driving genes of BLCA. scRNA-seq analysis of the somatic mutant alleles spectrum and clone structure of muscle infiltrating bladder urothelial cell carcinoma has identified four non-silent mutant alleles of *CFTR*, *NIPBL*, *ASTN1* and *DHX57* that might contribute to maintain the ancestral clones and the muscle invasion ability of subclones [18]. Furthermore, scRNA-seq has shed light on the potential origin of BLCA stem cells, which may be derived from non-stem cells within the bladder or bladder epithelial stem cells, and identified co-mutations of *ARID1A*, *GPRC5A*, and *MLL2* that can enhance the stem cell nature of BLCA [19].

Therefore, a series of bioinformatics analysis methods were used to screen the valuable somatic mutation-driven MRGs of BLCA, and the survival risk prediction model based on these potential biomarkers was established and verified. Meanwhile, the correlation analysis of immune cell infiltration, immune checkpoint and chemotherapeutic drug sensitivity were performed in this study. In addition, scRNA-seq data analysis revealed the changes in the expression of these biomarkers with the changes of epithelial cell status, and the key epithelial cell subsets that may affect

the prognosis of BLCA were identified. The goal of this study is to explore the mechanism and potential biomarkers of BLCA, and develop new therapeutic targets and approaches.

2. Materials and Methods

2.1 Data Collection

We downloaded the RNA-seq data of 433 BLCA patients from the TCGA database (<https://portal.gdc.cancer.gov/>) as training sets, of which 19 control samples and 414 tumour cases. 399 BLCA samples with complete survival information and 338 BLCA samples with somatic mutation data were retrieved. The GSE13507 and GSE135337 datasets were downloaded from the GEO database (<http://www.ncbi.nlm.nih.gov/geo/>). GSE13507 dataset, including 165 BLCA cases with survival information, was used as a validation set. The GSE135337 dataset incorporated scRNA-seq data of 7 BLCA samples. And 2751 MRGs were obtained from literature reports [20].

2.2 Identification of DEMRGs and Functional Enrichment Analyses

The expression matrix of 2751 MRGs was extracted from the TCGA-BLCA. The differentially expressed metabolism-related genes (DEMRGs) between normal and BLCA samples were screened using limma (version 3.48.3) [21] package in the R (version 4.2.3, University of Auckland, New Zealand). Based on $p < 0.05$ and $|\log_2FC| > 1$, the statistically significant DEMRGs were determined. The ggplot2 (version 3.3.5) was used to generate volcano plots to visualize gene expression data by plotting the \log_2 fold change on the x-axis and the negative \log_{10} of the p-value on the y-axis. Heatmaps of DEMRGs were performed using the heatmap (version 1.0.12) package. Moreover, the ClusterProfiler (version 4.0.2) was used to perform Gene Ontology (GO) and Kyoto Encyclopedia of Genes and Genomes (KEGG) analyses, and only results with a significance level of $p < 0.05$ were considered significant [22]. The GO analysis yielded three main categories: molecular function (MF), biological process (BP), and cellular component (CC) [23].

2.3 Construction of Prognostic Model

Firstly, the mutation frequency of DEMRGs was calculated using maftools package (Version 2.8.05) [24] according to TCGA-BLCA somatic mutation data. 399 BLCA samples with complete survival information from the TCGA-BLCA were randomly assigned to a training set of 279 cases and a test set of 120 cases. Survival package (Version 3.2-13) in R was used to perform univariate and multivariate COX proportional risk regression analysis. The COX model is used to evaluate whether the mutated DEMRGs were associated with patient survival. R package forestPlot (Version 1.10) was used to draw COX

forest plots. The mutated DEMRGs that were found to be associated with BLCA patients were then used as prognostic biomarkers.

We developed a risk models for BLCA patients using the predict.coxph function of survival package. The risk score we had calculated using this model is based on the patient's clinical and demographic variables, represented by X_1 to X_n . The coefficients (β_1 to β_n) were derived from the COX model and represent the effect of each variable on the risk of death. The prognostic formula was as follows: $Riskscore = h_0(t) \times \exp(\beta_1 X_1 + \beta_2 X_2 + \dots + \beta_n X_n)$. The Hazard Ratio (HR) value was obtained by exponentiating the coefficient and represented the ratio of the hazard rates between two groups of patients with different levels of the corresponding variable. The baseline hazard function $h_0(t)$ was a function of time that represents the risk of death due to BLCA in the absence of any other variable. By dividing the patients into high- and low-risk groups based on the median risk score, we identified the BLCA patients who are more likely to experience poor outcomes.

2.4 Validation of the Prognostic Risk Model

We employed the ggplot2 to generate risk curves and heat maps for two groups, survminer (version 0.4.9) to assess the correlations between the groups through K-M survival curves, and survivalROC package (version 1.0.3) to plot Receiver Operating Characteristic (ROC) curves for survival time points. We next verified the models applicability by repeating these analyses on a test set and GSE13507 validation dataset. Finally, we calculated mutation frequency of biomarkers to illustrate the importance of biomarkers in diseases.

2.5 Independence Prognostic of the Risk Model

The difference between the prognostic risk score and clinical traits (age, stage, gender, T-pathologic, M-pathologic, N-pathologic) in 399 BLCA patients were evaluated. The clinical traits were presented in **Supplementary Table 1**. BLCA patients were divided into two groups based on their disease stages: non-muscle invasive bladder cancer (NMIBC) and muscle-invasive bladder cancer (MIBC). NMIBC included Tis, Ta and T1 stage and MIBC included T2, T3 and T4 stage. To more closely understand the differences of two groups in the different T-stages, Kaplan-Meier survival curves were plotted. Finally, based on independent prognostic indicators identified through Cox analysis, we constructed nomogram using RMS (version 6.2-0) and Regplot (version 1.1). The nomogram was then evaluated using the calibration curves of 1-, 3-, 5-year, which was used to observe deviations between predicted and actual survival rates.

2.6 GSEA

In order to further explore related signaling pathways and potential biological mechanisms, the enrich-

ment analysis for biomarkers was performed using ClusterProfiler and org.Hs.eg.db Bioconductor annotation data package (version 3.12.0), respectively. The GSEA enriched gene set files (GO: c5.go.v7.4.entrez.gmt, KEGG: c2.cp.kegg.v7.4.entrez.gmt) were acquired from the GSEA website (<http://www.gsea-msigdb.org/gsea/msigdb>). The GSEA was performed for all genes in two risk groups, the threshold was set to $|NES| > 1$, $NOM\ p < 0.05$, $q < 0.05$. The top 10 GO enrichment biological process and the KEGG pathway were plotted using enrichplot packages (version 1.12.3).

2.7 Immune Checkpoint and Immune Microenvironment Analysis

The ICI of targeting immune checkpoints can upgrade the therapeutic efficacy of tumors. The conventional immune checkpoints CD274(PD-L1), CTLA-4(CTLA4), LAG-3(LAG3), LGALS(GAL9), HAVCR2(TIM3), PDCD1(PD-1), PDCD1LG2(PD-1LG2), and TIGIT(TIGIT) on patient survival were analyzed, and the K-M curves were plotted using survminer. We then used the ggplot2 to plot the checkpoints expression in two risk groups. In addition, we used the corrplot package (Version 0.92) to display the correlation between immune checkpoint and risk score. Ultimately, the correlation of 22 immune cells was investigated using the corrplot package. The CIBERSORT calculated the proportions of tumor infiltrating immune cells, and then the proportion of immune cells in two risk groups was plotted through the vioplot (version 0.3.7).

2.8 Sensitivity Analysis of Anticancer Drug

According to the list of 198 drugs in Genomics of Drug Sensitivity in Cancer database (GDSC, <https://www.cancerrxgene.org/>), the oncoPredict package (Version 0.2) [25] was used to evaluate the chemotherapy response by the IC50 of each patient, and evaluated the response of two groups to anticancer drugs. The smaller the IC50 value of the drug, the stronger the ability of the drug to inhibit cell growth, the better the effect of cancer treatment.

2.9 Single-Cell Analysis of Biomarkers in BLCA

The Seurat (Version 4.10) package [26] was used to conduct quality control of scRNA-seq data in the GSE135337 dataset. The low quality cells were removed to obtain the core cells, the anova was then performed. The core cells gene expression were normalized. The analysis of available dimensions were used using the JackStraw and ScoreJackStraw function. The dimension reduction was executed for the principal component using the tSNE algorithm. Then FindAllMarkers were used to identify biomarkers in each cluster, with min.pct = 0.2 and only.pos = TRUE, and Wilcoxon rank sum test was used to identify differential genes. SingleR (Version 1.6.1) was used to annotate different clusters in CellMarker database. Pseudo-

Table 1. Quantitative real-time PCR primers.

| Gene name | Forward primer | Reverse primer |
|----------------|-------------------------|-------------------------|
| <i>ABCC4</i> | GGCATACAAAGCAGAAGAGAGG | AAGGCAACGATGATGACAAACA |
| <i>FASN</i> | ACTTGCAGGAGTTCTGGGACAA | CTCGGAGTGAATCTGGGTTGAT |
| <i>ATP2B4</i> | CAATGAAATCAACTCCGAAAG | CAATGAAGAGACACCACAGCCA |
| <i>ATP8B2</i> | TTCCTGTTCCCTCCTCATTCTGC | TTCACCTGGTTATCGCTCTTGT |
| <i>MTHFD1L</i> | AGAGAGGCTGCGAGTAAAAGAAG | TGGTGAGATAGAGAAAGGTGGGT |
| <i>GAPDH</i> | ACAACCTTGGTATCGTGGAAGG | GCCATCACGCCACAGTTTC |

time and heat map of linear differentiation process were analyzed using the `plot_genes_in_pseudotime` function of Monocle package (version 2.20.0) [27]. Then, Consensus-ClusterPlus (Version1.56.0) [28] was used for synonymous clustering analysis. Finally, we made statistics on the number of interaction ligand receptors and polymers among different cell subtypes. The comprehensive and systematic analysis of communication molecules was conducted using the CellPhoneDB dataset. CellPhoneDB was used to analyze cell-to-cell communication networks and identify key cell-cell communication pathways in complex biological systems, gain insights into the various types of communication molecules involved in cell-to-cell interactions, such as ligands and receptors, and the signaling pathways they activate.

2.10 Validation of the Gene Expression Level by qRT-PCR

We applied quantitative real-time polymerase chain reaction (qRT-PCR) to validate the expression level of biomarkers in carcinoma tissue and normal control of 10 patients. Informed consent was obtained from all participants prior to enrollment into the study. And study protocols were approved by the Clinical Research Ethics Committees of the First Hospital of Shanxi Medical University ([2022](K056)). Total RNA was extracted using the Trizol reagent (Ambion company, Naugatuck, Connecticut, USA) according to the manufacturer. The SureScript-First-strand-cDNA-synthesis-kit First-Strand cDNA Synthesis Kit (Servicebio company, Wuhan, China) was used for reverse transcription reaction. The qRT-PCR reactions were performed as follows: 95 °C pre denaturation for 1 minute, 40 cycles of 95 °C denaturation for 20 seconds, 55 °C annealing for 20 seconds, and 72 °C final extension for 30 seconds. The $2^{-\Delta\Delta C_t}$ method was used for normalizing and quantifying gene expression levels. Primer sequences were included in Table 1. *GAPDH* was used as an internal reference gene. GraphPad Prism version 5.0.0 (San Diego, California USA) was used for statistical analysis and graphing. p value < 0.05 was considered as significant.

3. Results

3.1 Identification of DEMRGs and Functional Enrichment Analyses

In total, 201 DEMRGs were obtained between normal and BLCA samples in the TCGA-BLCA dataset, with

93 up-regulated DEMRGs and 108 down-regulated DEMRGs (Fig. 1A). Heatmap of DEMRGs between normal and BLCA samples were shown in Fig. 1B. Then the KEGG pathway and GO function assessed the function of 201 DEMRGs ($p < 0.05$). The gene expression profiles of normal and BLCA samples were highlighted by the color-coding. We observed that the BLCA samples had a significantly different gene expression profile compare to normal samples, indicating that the gene expression patterns were altered in BLCA. And 201 DEMRGs were enriched to 477 GO BP, 47 GO CC, and 178 GO MF, including alcohol metabolic process, cellular modified amino acid metabolic process, transmembrane transporter complex, transporter complex, metal ion transmembrane transporter activity, ion channel activity, etc (Fig. 1C, **Supplementary Table 2**). 201 DEMRGs were enriched to 226 KEGG pathways, and the top 10 KEGG pathways were listed in Fig. 1D and **Supplementary Table 3**, including cGMP-PKG signaling pathway, purine metabolism, pancreatic secretion, arachidonic acid metabolism, tryptophan metabolism, etc.

3.2 Construction of a Risk Model

According to TCGA-BLCA somatic mutation data, 24 DEMRGs with mutation frequency >3% were screened (**Supplementary Fig. 1**). Univariate COX analysis was carried out to construct model ($p < 0.05$), and 6 genes (*ATP8B2*, *CACNA2D1*, *MTHFD1L*, *FASN*, *ABCC4*, *ATP2B4*) were obtained (Fig. 2A). Multivariate COX analysis was performed to further screen the genes and identified 5 prognostic biomarkers (*FASN*, *ATP8B2*, *ABCC4*, *ATP2B4*, *MTHFD1L*) for BLCA (Fig. 2B). Additionally, the ROC curve of five genes were plotted to check the diagnostic ability. The area under the curve (AUC) for each gene was >0.7 (Fig. 2C), indicating that each gene has good diagnostic ability for BLCA. Furthermore, the five genes were used to construct a model, and the AUC of was 0.97, which confirmed the effectiveness and agility of the model (Fig. 2D).

3.3 Validation of the Prognostic Risk Model

The risk curve and the heatmap of model genes expression of two groups were drawn. The expression of *ABCC4* in the low-risk group was higher and it had a HR <1, indicating that it might be a favourable factor in predicting patient outcomes. While *FASN*, *ATP8B2*, *ATP2B4*,

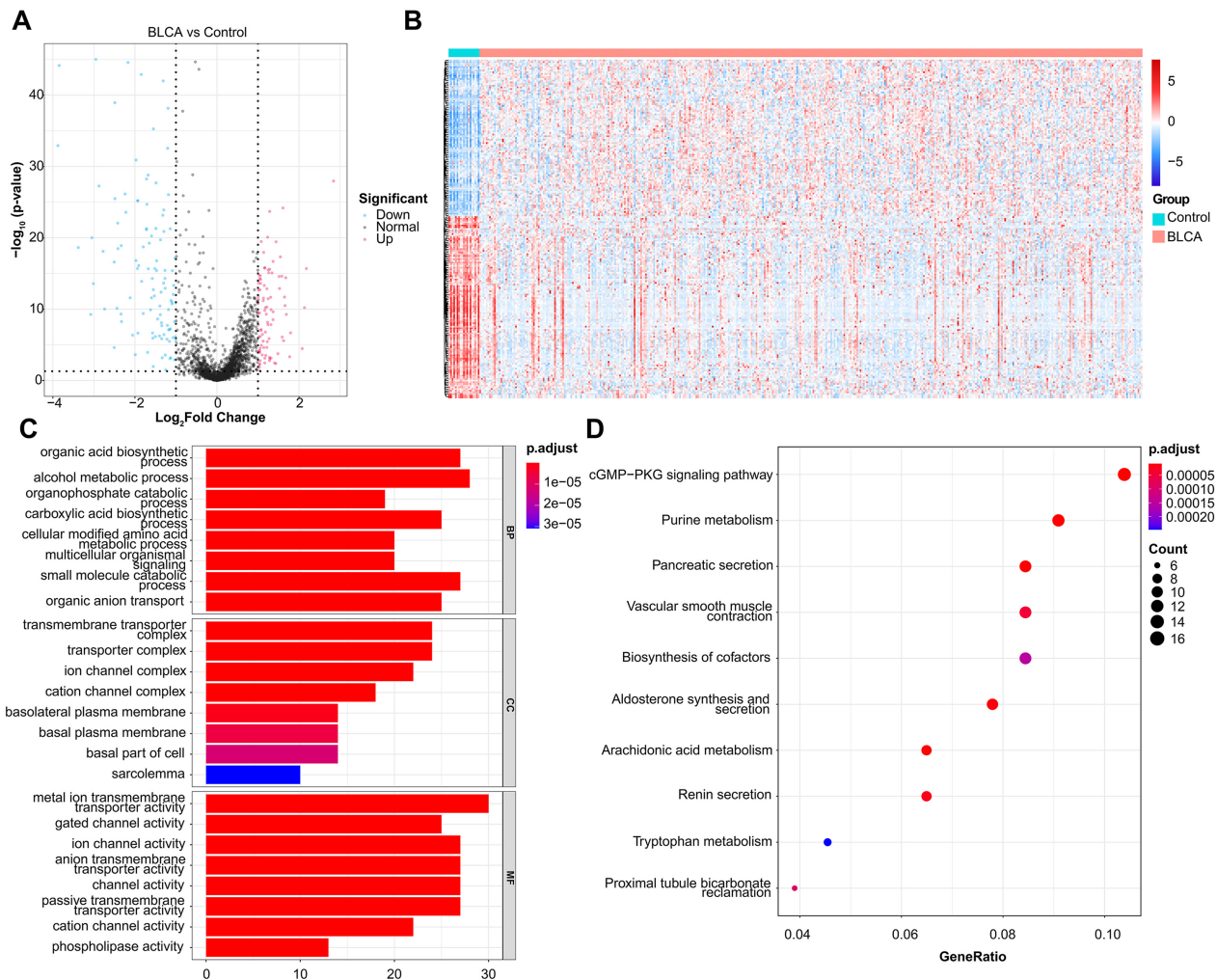


Fig. 1. DEMRGs screening and functional enrichment analysis. (A) Volcano plot of 201 DEMRGs. The value on x-axis represents the value of Log_2FC . Red dots represent up-regulated genes, while blue dots represent down-regulated genes. (B) Heatmap of DEMRGs. The up-regulated DEMRGs are shown in red, while the down-regulated DEMRGs are shown in blue. (C) GO biological process enrichment analysis. (D) KEGG pathway enrichment analysis.

MTHFD1L were risk factors as they had $\text{HR} > 1$, and they were highly expressed in high-risk group in the training set (Fig. 3A). The Kaplan-Meier curves showed that the cases in the high-risk group had worse survival compared to low-risk group (Fig. 3B). Furthermore, the ROC curves showed the 1–5 year AUCs were both > 0.6 (Fig. 3C). Subsequently, the prognosis of risk models were assessed in the test set and validation set. The gene expression patterns were consistent in the test set (Fig. 3D–F), validation set (Fig. 3G–I) and training set. In addition, the mutation frequency was calculated in different groups, the mutation frequency of biomarkers was greater than 8% in all mutant samples and the type of mutation was increased in the high-risk group (Supplementary Fig. 2).

3.4 Independence Prognostic of the Risk Model

The correlation result indicated there were significant differences in prognostic risk scores and clinical traits

(Fig. 4A). The results of K-M survival curves in T stage indicated that there were significant survival differences between two groups at pathological T2, T3, T4 stage (Fig. 4B). The Pvalue of all clinical factors was less than 0.05 except gender (Fig. 4C). And riskScore, T-pathologic, age, and N-pathologic were regarded as independent prognostic indicators using multivariate Cox analysis (Fig. 4D). Meanwhile, the nomogram and calibration curves were shown in Fig. 4E,F. And the nomogram C index was 0.7287, indicating the model had good predictive ability.

3.5 GSEA Functional Enrichment Analysis

We performed the GSEA method and acquired 90 GO biological process and 6 KEGG pathways to further validate the function. The top 10 GO enrichment BP and KEGG pathway were shown and the mainly GO terms enriched were GOLGI_APPARATUS, OXIDATIVE_PHOSPHORYLATION, RESPIRASOME, etc.

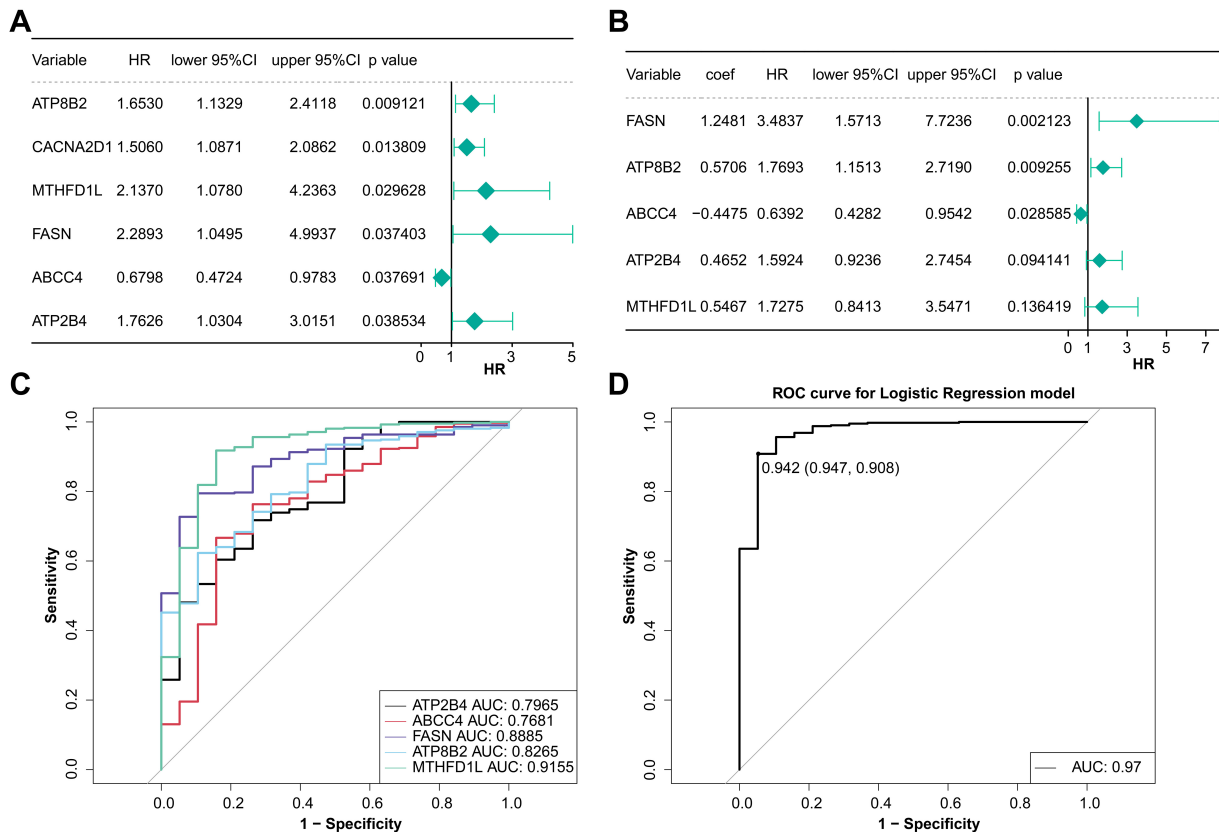


Fig. 2. Analysis of model genes in BLCA. (A) Univariate Cox regression analysis of prognostic genes. (B) Multivariate Cox regression analysis of prognostic genes. (C) The ROC curve of the diagnostic efficacy of single prognostic genes. (D) The ROC curve of the diagnostic efficacy of model gene.

(**Supplementary Fig. 3A**). The mainly KEGG pathways enriched were STEROID_HORMONE_BIOSYNTHESIS, OXIDATIVE_PHOSPHORYLATION, HUNTINGTONS_DISEASE, *etc.* (**Supplementary Fig. 3B**).

3.6 Immune Microenvironment and Immune Checkpoint Analysis

The correlation was analyzed to demonstrate the interaction of cell infiltrates in the immune microenvironment (Fig. 5A). The analysis of 22 immune cells population found that 4 immune cells had significantly different proportions. These 4 types of immune cells were B cells memory, Macrophages M0, Dendritic cells resting, and T cells (Fig. 5B). Moreover, the K-M survival curves analysis indicated that the immune checkpoint of LGALS9, PDCD1, and TIGHT had significant differences in two groups (Fig. 5C). And the expression level were analysis, the result indicated significant differences in expression levels of three immune checkpoints between the two groups (Fig. 5D). LGALS9 was significantly increased in low-risk group, while PDCD1, and TIGHT were significantly decreased. The correlation analysis results suggested that there are significant positive correlations between risk score and PDCD1 and TIGIF, and negative correlation between the risk score and LGALS9 (Fig. 5E).

3.7 Anticancer Drug Sensitivity Analysis

Among the 198 anticancer drug responses, 146 drugs were significantly different between two risk groups (**Supplementary Fig. 4A**). Patients were more sensitive to 42 drugs in the high-risk group, including 5-Fluorouracil_1073, Camptothecin_1003, Docetaxel_1819, *etc.* (**Supplementary Fig. 4B**). While patients were more sensitive to 104 drugs in the low-risk group, including Cisplatin_1005, Epirubicin_1511, Gemcitabine_1190, Vinblastine_1004, *etc.* (**Supplementary Fig. 4C**). All 198 drug list was shown in **Supplementary Fig. 4D**.

3.8 Single-Cell Analysis of Biomarkers in BLCA

The quality control of scRNA-seq was performed, and the results were showed in **Supplementary Fig. 5**. The core cells were screened, and 2000 genes whose expression levels had greatly difference were identified for subsequent analysis (**Supplementary Fig. 6**). PCA results showed that the overall distribution of sample cells was similar, and there were no outlier samples, and 15 principal components ($p < 0.05$) were screened for subsequent analysis (**Supplementary Fig. 7**). In addition, the p values of all core cells were less than 0.05, so all core cells were used for analysis. The clustering results suggested that core cells

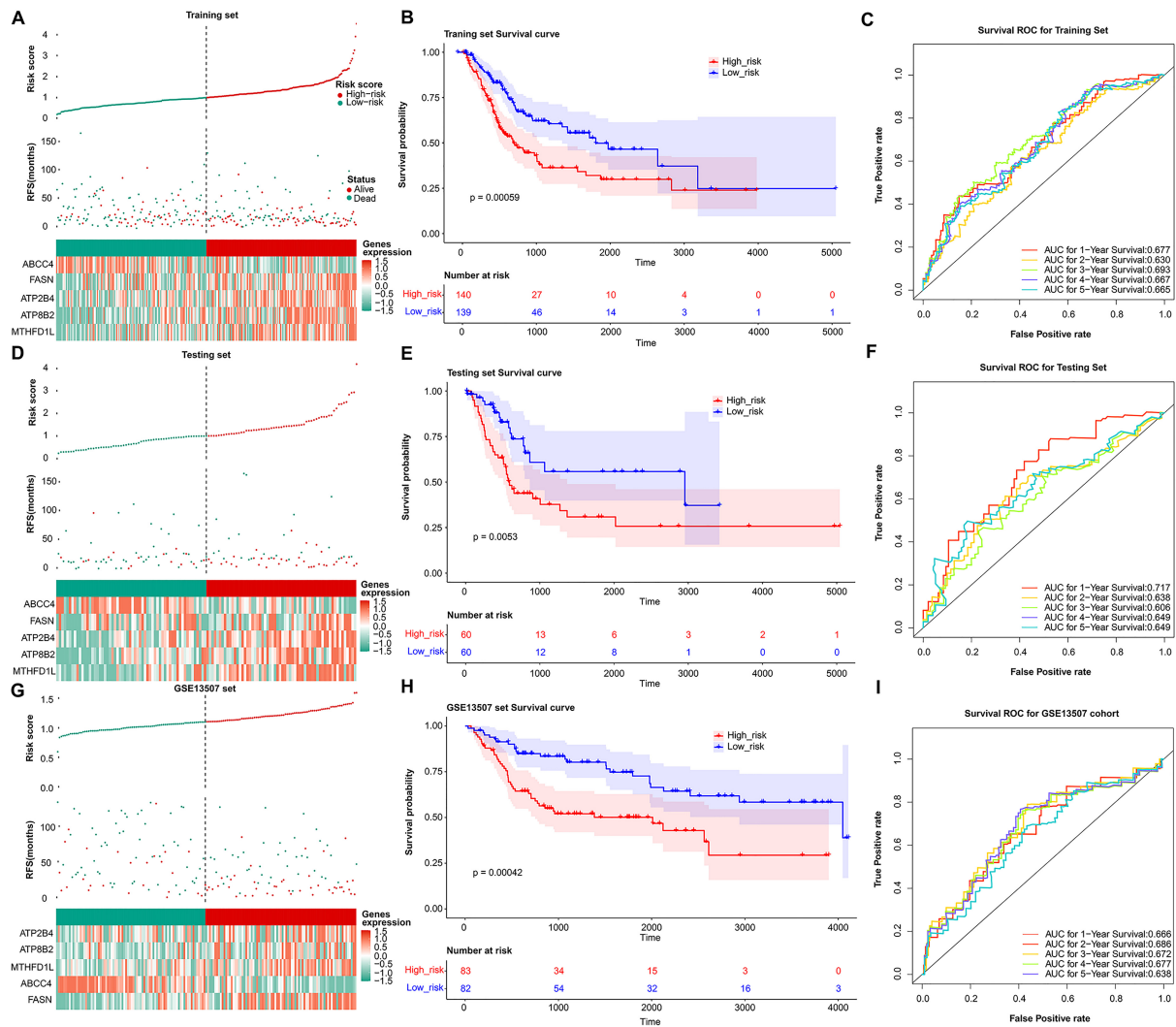


Fig. 3. Validation of the prognosis genes risk score system. The distribution of the risk score among BLCA patients in high- and low-risk groups, with green representing the number of survivors, and red representing the number of deaths; Heatmap of 5 prognosis genes expression profiles in high- and low-risk groups in the training set (A), test set (D), and validation set (G), separately. (B) Survival curves for high- and low-risk groups in the training set (B), test set (E), and validation set (H). ROC curves analysis of 1-, 2-, 3-, 4-, and 5-year predictions in the training set (C), test set (F), and validation set (I).

were segregated into 10 major distinct clusters (Fig. 6A). And the differential marker genes and the expression heat map were drawn of the top 10 marker genes in each cluster (Fig. 6B). The clusters included two types of cells with Epithelial_cells and DC (Fig. 6C). Because of the collected samples were epithelial cells and Dendritic cells (DC cells) accounted for a relatively small proportion, DC cells were removed for subsequent analysis. And the core cells were projected onto one root and two branches to construct a single cell track map (Fig. 6D). The expression changes of all biomarkers with trajectory changes were shown in Fig. 6E. The core cells of GSM4006644 sample in single-cell GSE135337 data set were spanned into two clusters based on their gene expression profiles. These clusters were named the low expression group (cluster 1) and high expression group (cluster 2) (Fig. 6F). Then, statistics

were made on cell types between the two groups. Cluster 2 and cluster 3 showed the greatest difference in the two groups (Fig. 6F,G). Furthermore, the cells of cluster 2 and cluster 3 were affected by other cluster cells, respectively (Fig. 6H).

3.9 Validation of the Gene Expression Level

We used qRT-PCR to further verify the expression level of the biomarkers (*ABCC4*, *FASN*, *ATP2B4*, *ATP8B2*, *MTHFD1L*) in normal control and carcinoma tissue of 10 patients. The qRT-PCR analysis showed that the expression level of these genes exhibited significant difference. The mRNA levels of *FASN* and *MTHFD1L* were significantly higher in carcinoma tissue, while *ABCC4*, *ATP2B4*, and *ATP8B2* were lower (Fig. 7).

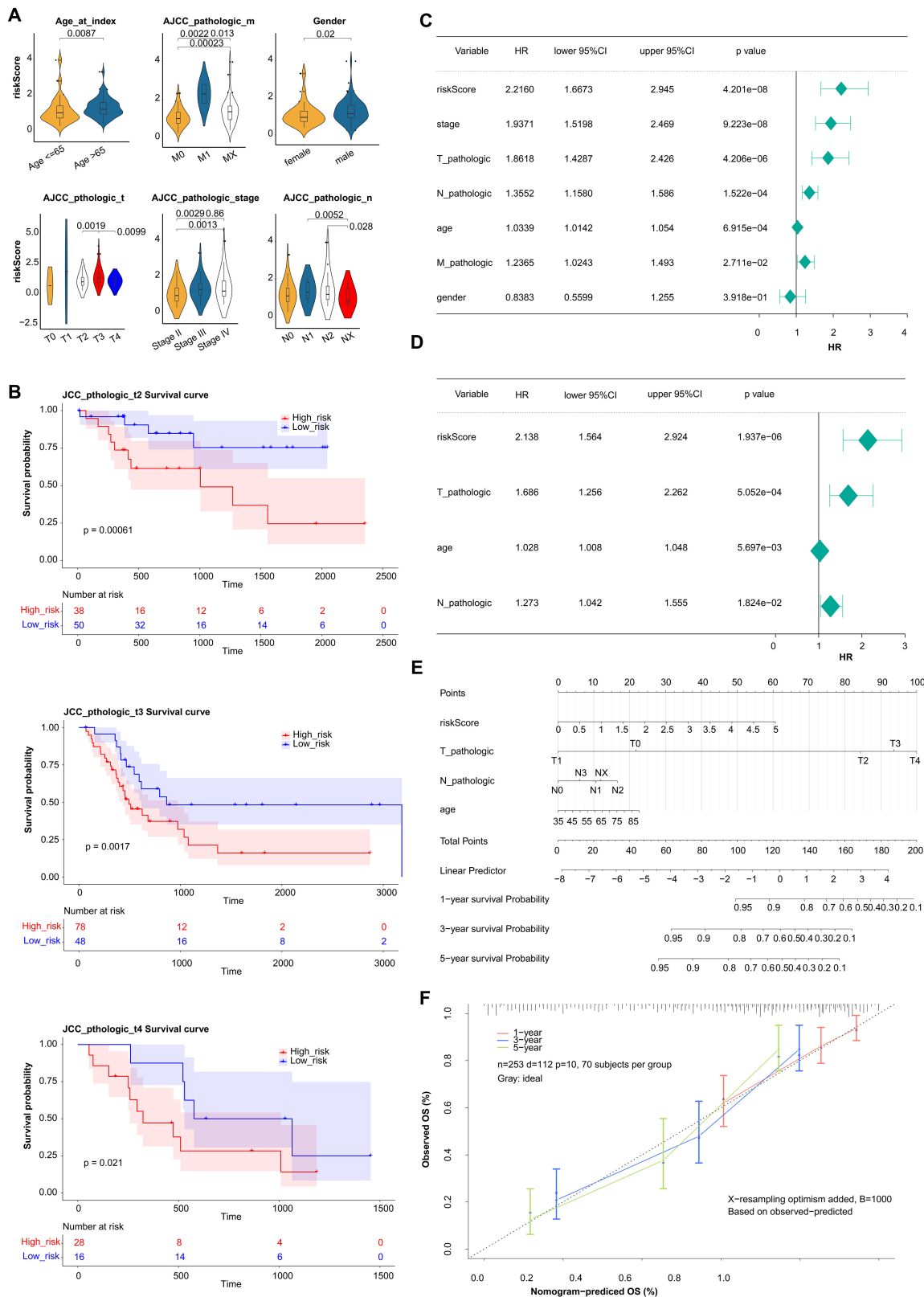


Fig. 4. Estimation of clinical Value of 5 prognostic genes in BLCA patients. (A) The correlation between the prognostic risk scores and clinical traits. (B) K-M survival curves in T stage between high- and low-risk groups. (C) Univariate Cox regression analysis of clinical traits. (D) Multivariate Cox regression analysis of clinical traits. (E) The nomogram of risk score and clinical traits to predict 1-, 3-, 5-year survival probability. (F) The calibration curves of the nomogram between predicted and observed 1-, 3-, and 5-year Overall Survival (OS).

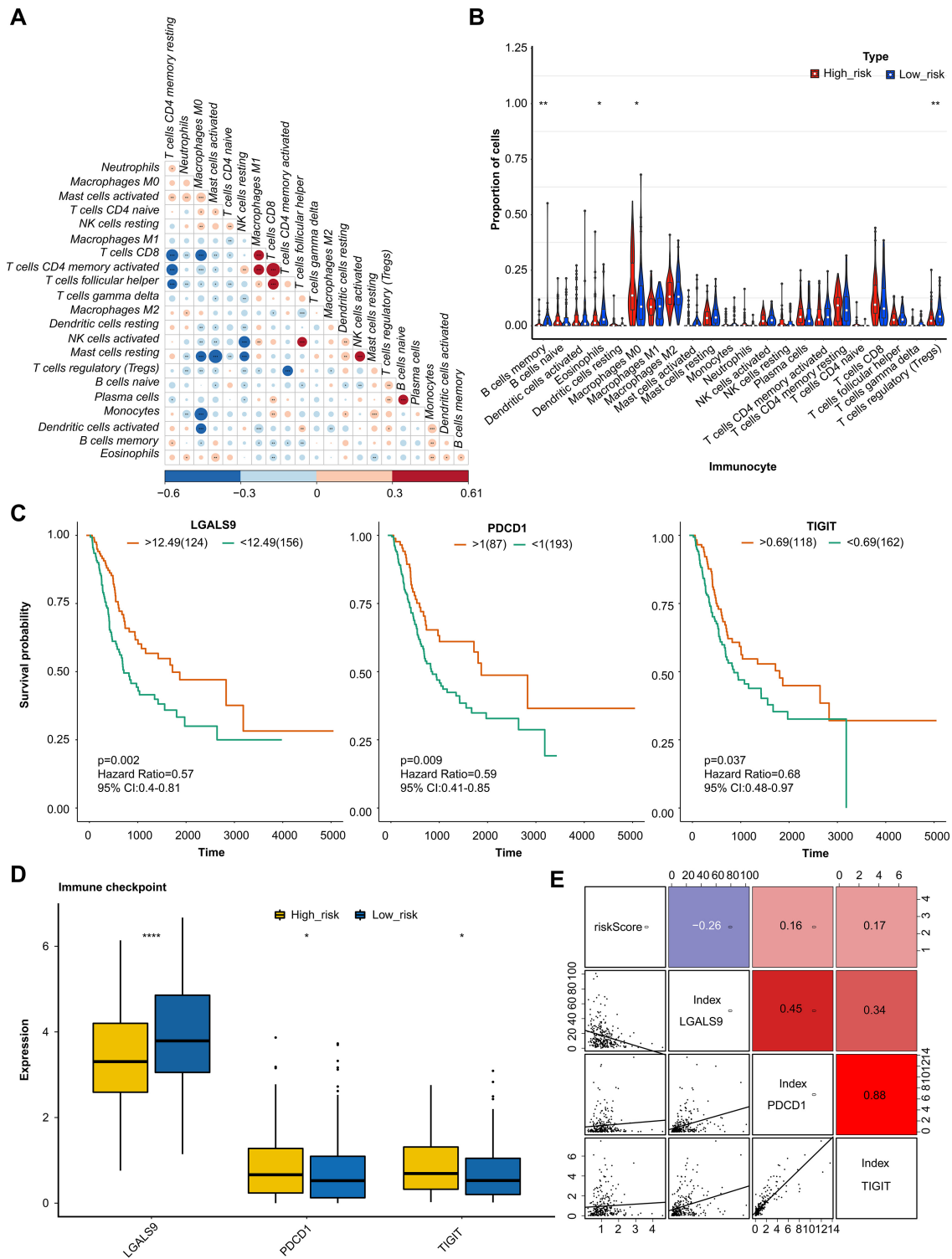


Fig. 5. Analysis of immune microenvironment and immune checkpoint. (A) Correlation analysis of immune cells examined the relationship between different types of immune cells present in the tumor microenvironment. (B) Proportion of immune cells by comparison of the percentage of different immune cells in high- and low-risk groups. (C) KM curve analysis of immune checkpoint showing the survival rates of patients in high- and low-risk groups, based on the expression of immune checkpoints. (D) Boxplot of immune checkpoint in high- and low-risk groups examined the distribution of immune checkpoints in the two groups. (E) Correlation analysis examined the relationship between the expression levels of immune checkpoints and risk values. The value bars without asterisk labeling are not significant, asterisk denotes statistically significant differences * $p \leq 0.05$; ** $p < 0.01$; *** $p < 0.001$; **** $p < 0.0001$ in comparison with control group.

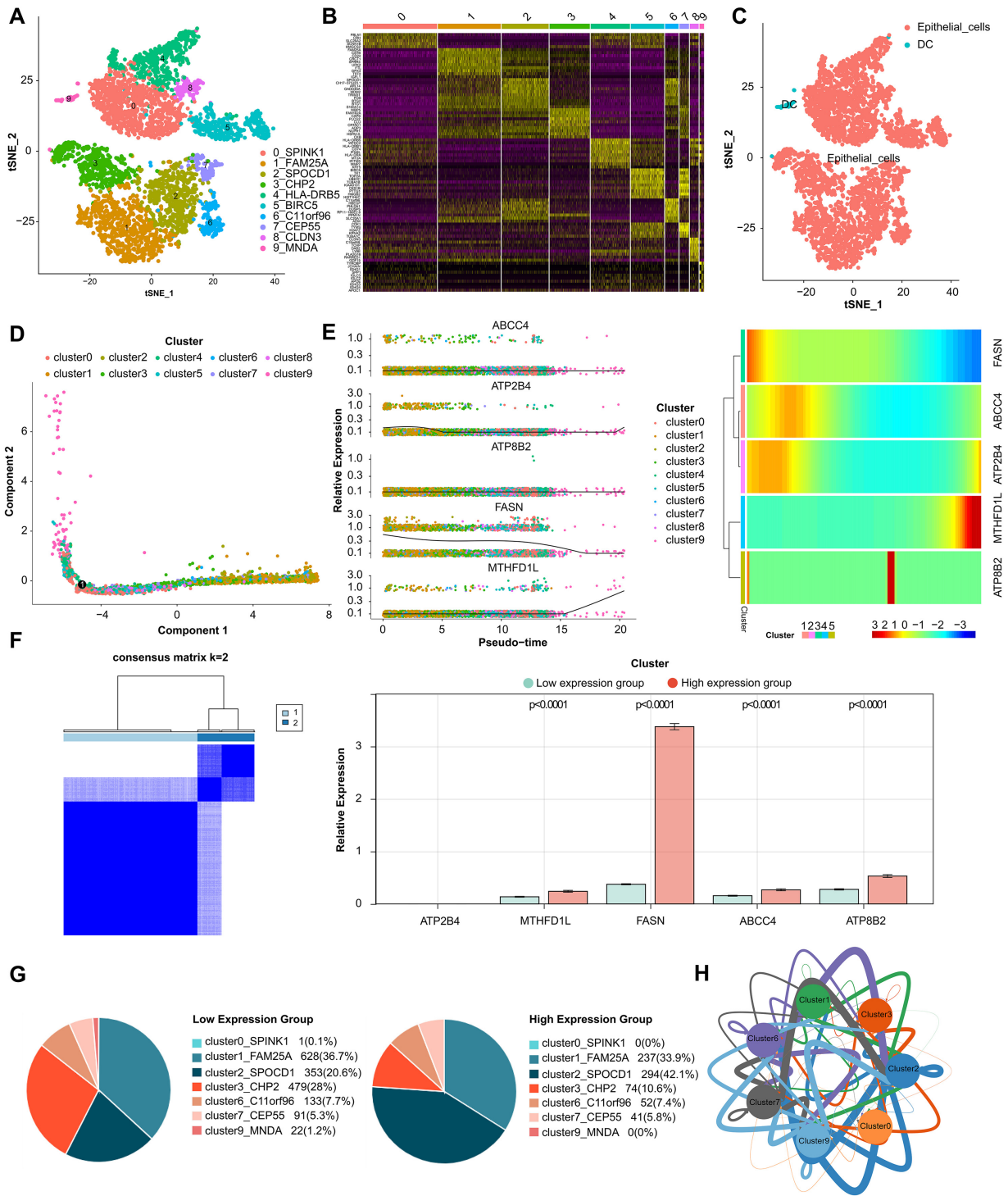


Fig. 6. Analysis of single-cell RNA sequencing. (A) Cells were clustered into 10 types and visualized in two dimensions using tSNE dimensionality reduction algorithm, and each color represented the annotated phenotype of each cluster. (B) The heatmap showed the top 10 marker genes of each cell cluster. Purple color indicates low expression of marker genes in each cell cluster, while yellow color indicates high expression. (C) The clusters of cells were annotated using singleR and CellMarker based on the composition of the marker genes. (D) Cell trajectory analysis diagram showed the differentiation trajectories of the cells. The cell tracks are epithelial cells. (E) The expression changes of a single gene and the heatmap of the expression levels of all genes in different differentiation trajectories of the pseudotime analysis. (F) Classification of high- and low-expression groups in core cells. (G) Percentage of cluster cells. (H) Interaction of clusters of cells.

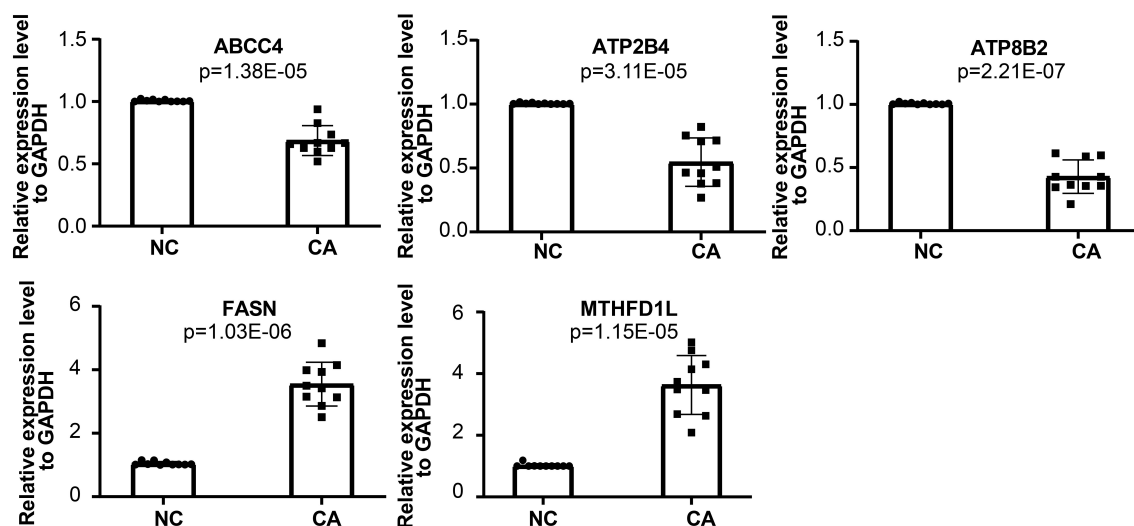


Fig. 7. qRT-PCR analysis of mRNA levels of *ABCC4*, *FASN*, *ATP2B4*, *ATP8B2*, and *MTHFD1L*.

4. Discussion

Over the years, the treatments of BLCA have made great progress, but the recurrence and progress of the disease after treatment still exists in a considerable number of patients, and once the disease progress will be a serious threat to the survival of patients. This may be closely related to the lack of good prognostic biomarkers to guide clinical decision-making. Studies have demonstrated that gene mutations and metabolic abnormalities are common and play an important role in various types of cancer, including lung cancer [29], prostate cancer [30], gastric cancer [31] and BLCA [32]. However, there are few studies on the relationship between gene mutation, metabolic abnormality and the prognosis of BLCA. We try to screen potential prognosis biomarkers and establish a reliable gene model by studying the MRGs of BLCA driven by somatic mutations, so as to provide basis for identifying new therapeutic targets and pathways of BLCA.

The functional enrichment results revealed that the differential MRGs of BLCA was mainly involved in the process of organic acid biosynthesis, small molecular catabolism, cell-modified amino acid metabolism, alcohol metabolism, signal transduction in multicellular organisms, organic anion transport, *etc.* We pay particular attention to the abnormal biosynthesis of organic acids has been implicated in the regulation of the growth and proliferation of cancer cells [33]. In cancer cells, the increased rate of glycolysis leads to the accumulation of large amount of lactic acid, which can prevent the hydroxylation of N-myc downstream regulatory protein of NMyC (NDRG3) by proline hydroxylase 2 (PHD2). The accumulation of NDRG3 activates RAF/ERK signaling pathway, which promotes angiogenesis and proliferation of cancer cells, allowing them to survive and adapt to the hypoxic microenvironment [34]. In addition, the changes of fatty acid synthe-

sis metabolism are related to the occurrence and development of BLCA. Silencing the expression of fatty acid synthase FASN can significantly inhibit the proliferation and invasion of BLCA cells through AKT/mTOR signal pathway [35]. Based on the TCGA-BLCA somatic mutation and Cox analyses, we identified five prognostic biomarkers (FASN, ABCC4, ATP2B4, ATP8B2, MTHFD1L) and developed a risk model for predicting the prognostic of BLCA with somatic mutation. The validation using independent test set, validation set and training set and found that these five genes were significantly associated with patient survival and were used to develop the prognostic risk model.

Immune system plays a critical roles in cancer development and progression, including BLCA. Studies have indicated that immune cell infiltration in BLCA is associated with the occurrence and progression of BLCA. Accordingly, we carried out the correlation analysis of immune microenvironment, and discovered that the activation levels of memory B cells, Treg cells, and dendritic cells were significantly increased in the low-risk group, while the activation level of macrophages was enrich in the high-risk group. Among them, B cells activate T cells mainly through antigen presentation and cytokine secretion, thus playing an anti-tumor immune role [36–38]. Dendritic cells in the tumor environment usually exhibit inhibitory and dysfunctional phenotypes, which help cancer cells escape host immune surveillance [39]. Although most studies have confirmed that the degree of Treg infiltration is negatively correlated with the survival rate of BLCA patients, different studies have pointed out that Treg may reduce the invasiveness of tumor cells by inhibiting the expression of invasive factor MMP-2 in BLCA cells and TAMs, resulting in Treg playing a good prognostic role in BLCA [40]. It is well known that macrophages undergo phenotypic transformation in tumor microenvironment, thus inhibiting anti-tumor immune response. Studies have shown that the contin-

uous infiltration of tumor-related inhibitory macrophages can significantly reduce the efficacy of BCG, and inhibitory macrophages expressing CD163 can be used as predictors of BCG unresponsive NMIBC [41,42]. Nevertheless, the correlation between the prognosis of BLCA and immune cell infiltration is very complex and unclear, so we need to do a lot of in-depth research.

In recent years, immune checkpoint inhibitors have shown strong anti-tumor activity in patients with locally advanced and metastatic BLCA [43]. Our study discovered that, in contrast, the expression level of PDCD1 and TIGIT in the routine immune checkpoint was higher in the high-risk group, while the expression level of LGALS9 was higher in low-risk group, suggesting that the gene expression and immune environment of the immune checkpoint are different in different risk groups. Patients may benefit from different types of immunotherapy with specific target. Chemotherapy is indeed a crucial treatment for BLCA and is often used in combination with other treatment such as surgery and radiation therapy [44]. Our results revealed that the low-risk group might be more sensitive to commonly used chemotherapy drugs for BLCA such as cisplatin, gemcitabine, vinblastine and epirubicin. On the other hand, the high-risk group was found to be not sensitive to intracavitary chemotherapy and arteriovenous chemotherapy. It may be necessary to adjust the medication regimen and choose more sensitive chemotherapeutic drugs, such as 5-fluorouracil, docetaxel, hydroxycamptothecin and so on.

Tumor drug resistance and tumor metastasis are major challenges in the treatment of advanced BLCA patients. By analyzing cell type-specific transcriptome variation by scRNA-seq, a personalized method for recurrent or refractory cancer has been developed, which is expected to overcome tumor drug resistance [45]. Tanaka *et al.* [46] found a new gene COX7B and its alternative marker CD63 related to platinum resistance by scRNA-seq. Low COX7B level was significantly correlated with poor chemotherapy response to BLCA [46]. Our study also attempts to use scRNA-seq data sets for further correlation analysis. We identified 10 BLCA epithelial cell subsets expressing different marker genes, and showed changes in the expression of five prognostic biomarkers (FASN, ABCC4, ATP2B4, ATP8B2, MTHFD1L) in different differentiation trajectories in pseudo-sequential analysis. Based on this, we found two cell clusters marked by SPOCD1 and CHP2, and their cell proportions changed significantly in the high and low expression groups of biomarkers. Moreover, it interacts with other cell clusters through cell communication and communication network, which not only further verifies the reliability of our survival risk stratification model, but also infers that these two cell clusters may affect the prognosis of BLCA and the key epithelial cell subsets that need our in-depth study.

In addition, combined with our research and previous reports, we have a better understanding of the above five

potential prognostic biomarkers of BLCA. FASN is a vital biological enzyme that can catalyze the reduction of acetyl-CoA (CoA) and malonyl-CoA to long-chain fatty acids by NADP [47]. FASN is an enzyme that plays a crucial role in the biosynthesis of fatty acids. Its up-regulation in many cancer types has been shown to be involved in the maintenance of cellular metabolism, division and proliferation [11]. Some studies have demonstrated that the increased FASN is markedly associated with the recurrence, progression, shorter RFS and poor PFS of BLCA [48,49]. This is consistent with our results. Moreover, inhibition of FASN can restrain the migration of bladder transitional cell carcinoma by activating AKT pathway [35].

ABCC4 is widely expressed in various tissues [50–52], and can actively transport a series of organic anions to extracellular, so most of the functional studies on ABCC4 are focused on its effect on cancer chemotherapy [53]. Previous studies have found that ABCC4 is related to drug resistance in various types of cancer, including breast cancer, colorectal cancer, prostate cancer, pancreatic cancer, and lung cancer [54–56]. Nonetheless, other studies have uncovered that low expression of ABCC4 can lead to the accumulation of cAMP in cells, which increases the invasiveness and migration of cancer cells [57]. Similarly, our results found that ABCC4 expression was significantly lower in the high-risk group, which had a higher risk of BLCA progression and metastasis. which needs to be confirmed by follow-up experimental study.

ATP2B4, the plasma membrane calcium ATP enzyme 4 (PMCA4), participates in the transport of divalent calcium ions out of the cell and maintains intracellular calcium homeostasis. It plays an important role in many diseases, including malaria, cardiomyopathy and cancer [58–60]. Previous study shows the evidence that changes in the expression levels of genes related to calcium pumps and calcium channels, including ATP2B4, may be a biomarker of cancer [61]. For example, the overexpression of ATP2B4 gene can promote the progression of colon cancer through intracellular calcium outflow [62]. Our results also show that the up-regulated expression of ATP2B4 may indicate a higher risk of disease progression in BLCA.

The ATP8B2 gene encodes an ATP-dependent phosphatidylcholine transferase that uses ATP as a source of energy to transport metals, ions and phospholipids across the cell membrane. At present, it has been discovered that ATP8B2 is related to various pathophysiological conditions in mouse models, but there are few reports on its relationship with human diseases. Through bioinformatics analysis, it has been found that ATP8B2, as a gene related to phenotypic transformation of macrophages, is related to the poor prognosis of pancreatic cancer [63]. Our results suggest that the expression level of ATP8B2 may serve as a prognostic biomarker for BLCA. Patient with higher expression of ATP8B2 and high risk of BLCA may have a poorer prognosis.

Methylenetetrahydrofolate dehydrogenase 1 (MTHFD1L) is an enzyme that is primarily located in the mitochondria, and it participates in carbon molecule, purine, thymidine and methionine metabolism [64]. MTHFD1L-related folate metabolism disorders and their products have been implicated in the occurrence and progression of various cancers [65–69]. Overexpression of MTHFD1L has been shown to be significantly related to poor prognosis in various types of cancer, including BLCA, head and neck cancer (HNSC), renal papillary cell carcinoma (KIRP), lung adenocarcinoma (LUAD) and endometrial carcinoma (UCEC) [70], which is consistent with our findings. However, some people have confirmed that MTHFD1L contributes to the regulation the growth and invasion of BLCA [71].

One limitation of this study is the lack of animal *in vivo* and cell line *in vitro* experiments to validate their role and specific mechanisms of marker genes in BLCA. Follow-up studies are needed to address this limitation and further investigate the potential of these markers as therapeutic targets or prognostic biomarkers. By conducting more comprehensive studies, we can better understand the complex mechanisms underlying cancer and develop more effective strategies for cancer prevention and treatment.

5. Conclusions

In this study, a new prognostic prediction model was established and verified by comprehensive bioinformatics analysis, which revealed the expression, prognostic value and function of MRGs driven by somatic mutation in BLCA. The potential markers of immunotherapy and chemotherapy were predicted in BLCA. In addition, through scRNA-seq data analysis, we explored the changes in the expression of biomarkers with the change of epithelial cell status, and identified two key epithelial cell subsets that affect the prognosis of BLCA, which need our in-depth study. The main advantage of this study is to use traditional RNA-seq data and scRNA-seq data to analyze and identify the biological significance of MRGs driven by somatic mutation in BLCA.

Availability of Data and Materials

CGA-BLCA dataset was downloaded from the TCGA database (<https://portal.gdc.cancer.gov/>) as training sets, of which 19 control samples and 414 tumour cases. The GSE13507 and GSE135337 datasets were retrieved from the GEO database (<https://www.ncbi.nlm.nih.gov/geo/>).

Author Contributions

LW and XY—conceptualization; LJ, SH, and LW—methodology and software; LW and MX—resources; LW—writing-original draft preparation; XY—writing-review and editing; LJ and MX—visualization; XY—supervision and project administration; LW—funding ac-

quisition. All authors contributed to editorial changes in the manuscript. All authors read and approved the final manuscript. All authors have participated sufficiently in the work and agreed to be accountable for all aspects of the work.

Ethics Approval and Consent to Participate

The study was conducted in accordance with the Declaration of Helsinki, and approved by the Clinical Research Ethics Committees of the First Hospital of Shanxi Medical University ([2022](K056)). Informed consent was obtained from all subjects involved in the study.

Acknowledgment

We thank all the patients who provided the specimens for this study.

Funding

This research was funded by the Nature Science Foundation of Shanxi Province, grant number 202103021224412.

Conflict of Interest

The authors declare no conflict of interest.

Supplementary Material

Supplementary material associated with this article can be found, in the online version, at <https://doi.org/10.31083/j.fbl2810242>.

References

- [1] Antoni S, Ferlay J, Soerjomataram I, Znaor A, Jemal A, Bray F. Bladder Cancer Incidence and Mortality: a Global Overview and Recent Trends. *European Urology*. 2017; 71: 96–108.
- [2] Sung H, Ferlay J, Siegel RL, Laversanne M, Soerjomataram I, Jemal A, *et al*. Global Cancer Statistics 2020: GLOBOCAN Estimates of Incidence and Mortality Worldwide for 36 Cancers in 185 Countries. *CA: a Cancer Journal for Clinicians*. 2021; 71: 209–249.
- [3] Ghandour R, Singla N, Lotan Y. Treatment Options and Outcomes in Nonmetastatic Muscle Invasive Bladder Cancer. *Trends in Cancer*. 2019; 5: 426–439.
- [4] Leow JJ, Bedke J, Chamie K, Collins JW, Daneshmand S, Grivas P, *et al*. SIU–ICUD consultation on bladder cancer: treatment of muscle-invasive bladder cancer. *World Journal of Urology*. 2019; 37: 61–83.
- [5] Barone B, Calogero A, Scafuri L, Ferro M, Lucarelli G, Di Zazzo E, *et al*. Immune Checkpoint Inhibitors as a Neoadjuvant/Adjuvant Treatment of Muscle-Invasive Bladder Cancer: A Systematic Review. *Cancers (Basel)*. 2022;14: 2545.
- [6] Valenza C, Antonarelli G, Giugliano F, Aurilio G, Verri E, Briganti A, *et al*. Emerging treatment landscape of non-muscle invasive bladder cancer. *Expert Opinion on Biological Therapy*. 2022; 22: 717–734.
- [7] Baldauf A, Koch R, Heberling U, Thomas C, Froehner M. Re: J. Alfred Witjes, Harman Max Bruins, Richard Cathomas, *et al*. European Association of Urology Guidelines on Muscle-invasive and Metastatic Bladder Cancer: Summary of the 2020

- Guidelines. *Eur Urol* 2020;79:82–104. *European Urology*. 2021; 79: e29.
- [8] Kroemer G, Pouyssegur J. Tumor Cell Metabolism: Cancer's Achilles' Heel. *Cancer Cell*. 2008; 13: 472–482.
- [9] Pavlova N, Thompson C. The Emerging Hallmarks of Cancer Metabolism. *Cell Metabolism*. 2016; 23: 27–47.
- [10] Hanahan D, Weinberg R. Hallmarks of Cancer: the next Generation. *Cell*. 2011; 144: 646–674.
- [11] Currie E, Schulze A, Zechner R, Walther T, Farese R. Cellular Fatty Acid Metabolism and Cancer. *Cell Metabolism*. 2013; 18: 153–161.
- [12] Chen X, Guo Y, Ouyang T, Li J, Wang T, Fan Z, *et al*. Co-mutation of TP53 and PIK3CA in residual disease after neoadjuvant chemotherapy is associated with poor survival in breast cancer. *Journal of Cancer Research and Clinical Oncology*. 2019; 145: 1235–1242.
- [13] Stachowiak M, Szymanski M, Ornoch A, Jancewicz I, Rusetzka N, Chrzan A, *et al*. SWI/SNF chromatin remodeling complex and glucose metabolism are deregulated in advanced bladder cancer. *IUBMB Life*. 2020; 72: 1175–1188.
- [14] Pan Y, Liu G, Zhou F, Su B, Li Y. DNA methylation profiles in cancer diagnosis and therapeutics. *Clinical and Experimental Medicine*. 2018; 18: 1–14.
- [15] Jiao F, Sun H, Yang Q, Sun H, Wang Z, Liu M, *et al*. Identification of FADS1 Through Common Gene Expression Profiles for Predicting Survival in Patients with Bladder Cancer. *Cancer management and research*. 2020; 12: 8325–8339.
- [16] Hao X, Luo H, Krawczyk M, Wei W, Wang W, Wang J, *et al*. DNA methylation markers for diagnosis and prognosis of common cancers. *Proceedings of the National Academy of Sciences of the United States of America*. 2017; 114: 7414–7419.
- [17] Wei W, Rong Y, Sanhe L, Chunxiu Y, Thokerunga E, Cui D, *et al*. Single-cell sequencing and its applications in bladder cancer. *Expert Reviews in Molecular Medicine*. 2022; 24: e6.
- [18] Li Y, Xu X, Song L, Hou Y, Li Z, Tsang S, *et al*. Single-cell sequencing analysis characterizes common and cell-lineage-specific mutations in a muscle-invasive bladder cancer. *GigaScience*. 2012; 1: 12.
- [19] Yang Z, Li C, Fan Z, Liu H, Zhang X, Cai Z, *et al*. Single-cell Sequencing Reveals Variants in ARID1a, GPRC5a and MLL2 Driving Self-renewal of Human Bladder Cancer Stem Cells. *European Urology*. 2017; 71: 8–12.
- [20] Wang Z, Embaye KS, Yang Q, Qin L, Zhang C, Liu L, *et al*. A Novel Metabolism-Related Signature as a Candidate Prognostic Biomarker for Hepatocellular Carcinoma. *Journal of Hepatocellular Carcinoma*. 2021; 8: 119–132.
- [21] Ritchie ME, Phipson B, Wu D, Hu Y, Law CW, Shi W, *et al*. Limma powers differential expression analyses for RNA-sequencing and microarray studies. *Nucleic Acids Research*. 2015; 43: e47.
- [22] Wu T, Hu E, Xu S, Chen M, Guo P, Dai Z, *et al*. ClusterProfiler 4.0: a universal enrichment tool for interpreting omics data. *The Innovation*. 2021; 2: 100141.
- [23] Ma M, Xie W, Li X. Identification of Autophagy-Related Genes in the Progression from Non-Alcoholic Fatty Liver to Non-Alcoholic Steatohepatitis. *International Journal of General Medicine*. 2021; 14: 3163–3176.
- [24] Mayakonda A, Lin D, Assenov Y, Plass C, Koeffler HP. Maftools: efficient and comprehensive analysis of somatic variants in cancer. *Genome Research*. 2018; 28: 1747–1756.
- [25] Maeser D, Gruener RF, Huang RS. oncoPredict: an R package for predicting *in vivo* or cancer patient drug response and biomarkers from cell line screening data. *Briefings in bioinformatics*. 2021; 22: bbab260.
- [26] Hao Y, Hao S, Andersen-Nissen E, Mauck WM, Zheng S, Butler A, *et al*. Integrated analysis of multimodal single-cell data. *Cell*. 2021; 184: 3573–3587.e29.
- [27] Trapnell C, Cacchiarelli D, Grimsby J, Pokharel P, Li S, Morse M, *et al*. The dynamics and regulators of cell fate decisions are revealed by pseudotemporal ordering of single cells. *Nature Biotechnology*. 2014; 32: 381–386.
- [28] Wilkerson MD, Hayes DN. ConsensusClusterPlus: a class discovery tool with confidence assessments and item tracking. *Bioinformatics*. 2010; 26: 1572–1573.
- [29] Sun Z, Jiang Q, Li J, Guo J. The potent roles of salt-inducible kinases (SIKs) in metabolic homeostasis and tumorigenesis. *Signal Transduction and Targeted Therapy*. 2020; 5: 150.
- [30] Liu RZ, Godbout R. An Amplified Fatty Acid-Binding Protein Gene Cluster in Prostate Cancer: Emerging Roles in Lipid Metabolism and Metastasis. *Cancers (Basel)*. 2020; 12: 3823.
- [31] Huang S, Guo Y, Li Z, Zhang Y, Zhou T, You W, *et al*. A systematic review of metabolomic profiling of gastric cancer and esophageal cancer. *Cancer Biology and Medicine*. 2020; 17: 181–198.
- [32] Cheng S, Wang G, Wang Y, Cai L, Qian K, Ju L, *et al*. Fatty acid oxidation inhibitor etomoxir suppresses tumor progression and induces cell cycle arrest via PPAR γ -mediated pathway in bladder cancer. *Clinical Science*. 2019; 133: 1745–1758.
- [33] Yuan Y, Li H, Pu W, Chen L, Guo D, Jiang H, *et al*. Cancer metabolism and tumor microenvironment: fostering each other? *Science China Life Sciences*. 2022; 65: 236–279.
- [34] Lee D, Sohn H, Park Z, Oh S, Kang Y, Lee K, *et al*. A Lactate-Induced Response to Hypoxia. *Cell*. 2015; 161: 595–609.
- [35] Zheng SS, Gao JG, Liu ZJ, Zhang XH, Wu S, Weng BW, *et al*. Downregulation of fatty acid synthase complex suppresses cell migration by targeting phospho-AKT in bladder cancer. *Molecular Medicine Reports*. 2016; 13: 1845–1850.
- [36] Sharonov GV, Serebrovskaya EO, Yuzhakova DV, Britanova OV, Chudakov DM. B cells, plasma cells and antibody repertoires in the tumour microenvironment. *Nature Reviews Immunology*. 2020; 20: 294–307.
- [37] Michaud D, Steward CR, Mirlekar B, Pylayeva-Gupta Y. Regulatory B cells in cancer. *Immunological Reviews*. 2021; 299: 74–92.
- [38] Wang S, Liu W, Ly D, Xu H, Qu L, Zhang L. Tumor-infiltrating B cells: their role and application in anti-tumor immunity in lung cancer. *Cellular and Molecular Immunology*. 2019; 16: 6–18.
- [39] Ma Y, Shurin GV, Peiyuan Z, Shurin MR. Dendritic Cells in the Cancer Microenvironment. *Journal of Cancer*. 2013; 4: 36–44.
- [40] Winerdal ME, Krantz D, Hartana CA, Zirakzadeh AA, Linton L, Bergman EA, *et al*. Urinary Bladder Cancer Tregs Suppress MMP2 and Potentially Regulate Invasiveness. *Cancer Immunology Research*. 2018; 6: 528–538.
- [41] Kardoust Parizi M, Shariat SF, Margulis V, Mori K, Lotan Y. Value of tumour-infiltrating immune cells in predicting response to intravesical BCG in patients with non-muscle-invasive bladder cancer: a systematic review and meta-analysis. *BJU International*. 2021; 127: 617–625.
- [42] Miyake M, Tatsumi Y, Gotoh D, Ohnishi S, Owari T, Iida K, *et al*. Regulatory T Cells and Tumor-Associated Macrophages in the Tumor Microenvironment in Non-Muscle Invasive Bladder Cancer Treated with Intravesical Bacille Calmette-Guérin: A Long-Term Follow-Up Study of a Japanese Cohort. *International Journal of Molecular Sciences*. 2017; 18: 2186.
- [43] Wu Z, Liu J, Dai R, Wu S. Current status and future perspectives of immunotherapy in bladder cancer treatment. *Science China Life Sciences*. 2021; 64: 512–533.
- [44] Liu S, Chen X, Lin T. Emerging strategies for the improvement of chemotherapy in bladder cancer: Current knowledge and future perspectives. *Journal of Advanced Research*. 2022; 39: 187–202.
- [45] Lee HW, Chung W, Lee H, Jeong DE, Jo A, Lim JE, *et al*.

- Single-cell RNA sequencing reveals the tumor microenvironment and facilitates strategic choices to circumvent treatment failure in a chemorefractory bladder cancer patient. *Genome Medicine*. 2020; 12: 47.
- [46] Tanaka N, Katayama S, Reddy A, Nishimura K, Niwa N, Hongo H, *et al*. Single-cell RNA-seq analysis reveals the platinum resistance gene COX7B and the surrogate marker CD63. *Cancer Medicine*. 2018; 7: 6193–6204.
- [47] Kuhajda FP, Jenner K, Wood FD, Hennigar RA, Jacobs LB, Dick JD, *et al*. Fatty acid synthesis: a potential selective target for antineoplastic therapy. *Proceedings of the National Academy of Sciences of the United States of America*. 1994; 91: 6379–6383.
- [48] Jiang B, Li E, Lu Y, Jiang Q, Cui D, Jing Y, *et al*. Inhibition of Fatty-acid Synthase Suppresses P-AKT and Induces Apoptosis in Bladder Cancer. *Urology*. 2012; 80: 484.e9–484.e15.
- [49] Abdelrahman AE, Rashed HE, Elkady E, Elsebai EA, El-Azony A, Matar I. Fatty acid synthase, Her2/neu, and E2F1 as prognostic markers of progression in non-muscle invasive bladder cancer. *Annals of Diagnostic Pathology*. 2019; 39: 42–52.
- [50] Chan LMS, Lowes S, Hirst BH. The ABCs of drug transport in intestine and liver: efflux proteins limiting drug absorption and bioavailability. *European Journal of Pharmaceutical Sciences*. 2004; 21: 25–51.
- [51] Imaoka T, Kusuhara H, Adachi M, Schuetz JD, Takeuchi K, Sugiyama Y. Functional Involvement of Multidrug Resistance-Associated Protein 4 (MRP4/ABCC4) in the Renal Elimination of the Antiviral Drugs Adefovir and Tenofovir. *Molecular Pharmacology*. 2007; 71: 619–627.
- [52] Krishnamurthy P, Schwab M, Takenaka K, Nachagari D, Morgan J, Leslie M, *et al*. Transporter-Mediated Protection against Thiopurine-Induced Hematopoietic Toxicity. *Cancer Research*. 2008; 68: 4983–4989.
- [53] Wen J, Luo J, Huang W, Tang J, Zhou H, Zhang W. The Pharmacological and Physiological Role of Multidrug-Resistant Protein 4. *Journal of Pharmacology and Experimental Therapeutics*. 2015; 354: 358–375.
- [54] Huang H, Li J, Shen J, Lin L, Wu X, Xiang S, *et al*. Increased ABCC4 Expression Induced by ERR α Leads to Docetaxel Resistance via Efflux of Docetaxel in Prostate Cancer. *Frontiers in Oncology*. 2020; 10: 1474.
- [55] Sudhakaran M, Parra MR, Stoub H, Gallo KA, Doseff AI. Apigenin by targeting hnRNP2 sensitizes triple-negative breast cancer spheroids to doxorubicin-induced apoptosis and regulates expression of ABCC4 and ABCG2 drug efflux transporters. *Biochemical Pharmacology*. 2020; 182: 114259.
- [56] Sahores A, Carozzo A, May M, Gómez N, Di Siervi N, De Sousa Serro M, *et al*. Multidrug transporter MRP4/ABCC4 as a key determinant of pancreatic cancer aggressiveness. *Scientific Reports*. 2020; 10: 14217.
- [57] Kryczka J, Sochacka E, Papiewska-Pająk I, Boncela J. Implications of ABCC4-Mediated cAMP Efflux for CRC Migration. *Cancers (Basel)*. 2020; 12: 3547.
- [58] Lessard S, Gatof ES, Beaudoin M, Schupp PG, Sher F, Ali A, *et al*. An erythroid-specific ATP2B4 enhancer mediates red blood cell hydration and malaria susceptibility. *Journal of Clinical Investigation*. 2017; 127: 3065–3074.
- [59] Mohamed TMA, Abou-Leisa R, Stafford N, Maqsood A, Zi M, Prehar S, *et al*. The plasma membrane calcium ATPase 4 signalling in cardiac fibroblasts mediates cardiomyocyte hypertrophy. *Nature Communications*. 2016; 7: 11074.
- [60] Monteith GR, Davis FM, Roberts-Thomson SJ. Calcium Channels and Pumps in Cancer: Changes and Consequences. *Journal of Biological Chemistry*. 2012; 287: 31666–31673.
- [61] Monteith GR, McAndrew D, Faddy HM, Roberts-Thomson SJ. Calcium and cancer: targeting Ca²⁺ transport. *Nature Reviews Cancer*. 2007; 7: 519–530.
- [62] Geyik E, Ipci YZ, Pala E, Suner A, Borazan E, Bozgeyik I, *et al*. Investigation of the association between ATP2B4 and ATP5B genes with colorectal cancer. *Gene*. 2014; 540: 178–182.
- [63] Li MX, Wang HY, Yuan CH, Ma ZL, Jiang B, Li L, *et al*. Establishment of a Macrophage Phenotypic Switch Related Prognostic Signature in Patients With Pancreatic Cancer. *Frontiers in Oncology*. 2021; 11: 619517.
- [64] Cui L, Zhao X, Jin Z, Wang H, Yang S, Hu S. Melatonin modulates metabolic remodeling in HNSCC by suppressing MTHFD1L-formate axis. *Journal of Pineal Research*. 2021; 71: e12767.
- [65] Ali M, Lemonakis K, Wihlborg AK, Veskovski L, Turesson I, Mellqvist UH, *et al*. Sequence variation at the MTHFD1L-AKAP12 and FOPNL loci does not influence multiple myeloma survival in Sweden. *Blood Cancer Journal*. 2019; 9: 57.
- [66] He Z, Wang X, Zhang H, Liang B, Zhang J, Zhang Z, *et al*. High expression of folate cycle enzyme MTHFD1L correlates with poor prognosis and increased proliferation and migration in colorectal cancer. *Journal of Cancer*. 2020; 11: 4213–4221.
- [67] Do SK, Choi SH, Lee SY, Choi JE, Kang H, Hong MJ, *et al*. Genetic Variants in one-Carbon Metabolism Pathway Predict Survival Outcomes of Early-Stage Non-Small Cell Lung Cancer. *Oncology*. 2020; 98: 897–904.
- [68] Chen J, Yang J, Xu Q, Wang Z, Wu J, Pan L, *et al*. Integrated bioinformatics analysis identified MTHFD1L as a potential biomarker and correlated with immune infiltrates in hepatocellular carcinoma. *Bioscience Reports*. 2021; 41: BSR20202063.
- [69] Li H, Fu X, Yao F, Tian T, Wang C, Yang A. MTHFD1L-Mediated Redox Homeostasis Promotes Tumor Progression in Tongue Squamous Cell Carcinoma. *Frontiers in Oncology*. 2019; 9: 1278.
- [70] Sial N, Rehman J, Saeed S, Ahmad M, Hameed Y, Atif M, *et al*. Integrative analysis reveals methylenetetrahydrofolate dehydrogenase 1-like as an independent shared diagnostic and prognostic biomarker in five different human cancers. *Bioscience Reports*. 2022; 42: BSR20211783.
- [71] Eich M, Rodriguez Pena MDC, Chandrashekar DS, Chau A, Agarwal S, Gordetsky JB, *et al*. Expression and Role of Methylenetetrahydrofolate Dehydrogenase 1 Like (MTHFD1L) in Bladder Cancer. *Translational Oncology*. 2019; 12: 1416–1424.